Journal of
Materials Chemistry C

RSC Publishing

FEATURE ARTICLE

Advances in the synthesis of ZnO nanomaterials for varistor devices

Cite this: *J. Mater. Chem. C*, 2013, **1**, 3268

Suresh C. Pillai,*[a] John M. Kelly,[b] Raghavendra Ramesh[c] and Declan E. McCormack[ad]

ZnO based varistors are widely used for overvoltage protection in many electrical and electronic circuits, at voltages ranging from a few to over a million volts. By careful control of the microstructure, through nano-structuring by chemical routes, it should be possible to produce varistors with high breakdown voltage (V_c), as this is proportional to the number of active grain boundaries in the sintered body. This property is particularly important for the production of the small-sized varistors needed for modern electronic instruments such as tablet computers and mobile phones. The current review will outline the recent advances in the chemical processing (*e.g.* sol–gel, combustion synthesis plasma pyrolysis, micro-emulsion synthesis and precipitation routes) of varistors from ZnO nanomaterials and the properties of these materials. Uncontrolled grain growth at higher temperature is highlighted as a major challenge for obtaining desirable electrical properties for nano-varistors. Various novel sintering techniques such as step-sintering, spark plasma and microwave sintering methods are expected to deliver a varistor with controlled grain growth and optimum electrical characteristics.

Received 7th November 2012
Accepted 19th February 2013

DOI: 10.1039/c3tc00575e

www.rsc.org/MaterialsC

[a]*Center for Research in Engineering Surface Technology (CREST), FOCAS Institute, Dublin Institute of Technology, Kevin Street, Dublin 8, Ireland. E-mail: Suresh.pillai@dit.ie*

[b]*School of Chemistry, University of Dublin, Trinity College, Dublin 2, Ireland*

[c]*South Eastern Applied Materials Research Centre, Applied Technology Building, Waterford Institute of Technology, Waterford, Ireland*

[d]*School of Chemical and Pharmaceutical Sciences, Dublin Institute of Technology, Kevin Street, Dublin 8, Ireland*

Dr Suresh C. Pillai obtained his PhD in the area of Materials Science from Trinity College (TCD), The University of Dublin, Ireland and then performed a postdoctoral research at California Institute of Technology (Caltech), USA. Dr Pillai is an elected fellow of the Royal Microscopical Society (FRMS) and the Institute of Materials, Minerals and Mining (FIMMM). Dr Pillai was responsible for acquiring more than €2 million direct R&D funding. He has published several scientific articles in leading peer reviewed journals, has contributed four book chapters, has presented at more than twenty international conferences and has delivered over fifteen international invited talks. Dr Pillai is a recipient of a number of national awards for research accomplishments including the 'Industrial Technologies Award 2011' from Enterprise Ireland for commercialising nanomaterials for industrial applications.

Professor John M. Kelly obtained his B.Sc. from the University of Manchester in 1965, an M.Sc. in organic photochemistry from McMaster University (supervisor, John J. McCullough) and his PhD from the University of London (supervisor, George Porter) in 1970. After a Leverhulme Teaching Fellowship at the University of the West Indies, Jamaica, he carried out post-doctoral work in Ernst Koerner von Gustorf's group at the Max Planck Institut für Strahlenchemie, Mülheim. He joined Trinity College Dublin in 1973 and was Head of Department from 1994–2000. He is a Fellow of the Royal Society of Chemistry and a Member of the Royal Irish Academy (MRIA). Research interests include the transient spectroscopy and photochemistry of DNA and metal-containing compounds and the synthesis of micro- and nano-particles of metals and metal oxides for applications in electronic devices and biosensors.

Introduction

ZnO varistors are solid-state electronic ceramic components whose key function is to sense and limit transient voltage surges (short duration spikes in voltage).[1–10] A sudden variation in the electrical condition of circuits arising from lightning strikes, electro-static discharge, *etc.* would cause a transient voltage to be generated from the energy stored due to the circuit capacitance and conductance,[2] so that a key varistor attribute of transient overvoltage protection requires the impulse energy to be dissipated at a voltage low enough to guarantee the survival of the electrical components.[3–11]

The ZnO varistor was initially invented by Matsuoka in Japan[1] and has been available in the market since 1972. Zinc oxide varistors are widely known by various trade names such as voltage arrestors, surge suppressers, non-linear resistors, and voltage regulators or stabilisers. Some typical package styles of varistors that allow variation in energy ratings as well as in mechanical mounting for different user applications are shown in Fig. 1.

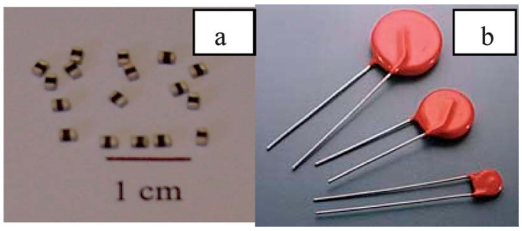

Fig. 1 Various types of ZnO varistors fabricated for different uses (a) varistors used in electronic circuits for ESD (Electro Static Discharge) low voltage suppression and protection (b) varistors used in industrial/AC line protection (*Reproduced with permission from* S. C. Pillai, J. M. Kelly, D. E. McCormack and R. Ramesh, *J. Mater. Chem.*, 2008, **18**, 3926).

Varistors are voltage dependent, non-ohmic devices whose electrical characteristics are almost similar to 'back-to-back Zener diodes'.[2] When exposed to a high voltage the varistor impedance varies from a near open circuit to a highly conductive state, thus clamping the transient voltage to a harmless level and protecting electronic components in expensive electronic devices.[2,4] A schematic *I–V* characteristic curve of a varistor is shown in Fig. 2.[2–10] (Note that varistor electrical characteristics are generally represented using log–log format in order to illustrate the wide range of its electrical operation).

As can be seen from the figure, the *I–V* characteristics of varistors can be classified into three distinct regions, *viz.*, pre-switch or leakage region, non-linear or varistor operation region and high current or upturn region.

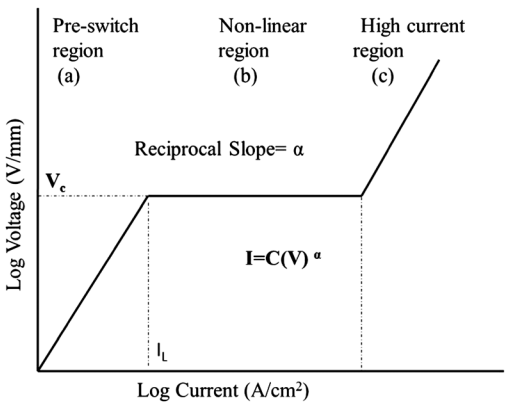

Fig. 2 Schematic *I–V* characteristic curve of an idealised varistor. (a) Leakage or pre-switch region, I_L leakage current; V_c, break-down voltage (b) non-ohmic or varistor operation region (c) High current or upturn region.

Dr Ramesh Raghavendra, holds a PhD from University of Twente, The Netherlands and three Master degrees (M.Sc., M.S, MBA). He worked for five years at University of Limerick as Senior Research Fellow and later as Senior Materials Technologist for a MNC in Dundalk for over 10 years prior to joining SEAM in 2008. His research background is in the areas of functional ceramics, glass and glass-ceramics. He holds two patents and has authored/co-authored more than 50 refereed journal publications. In his present role as centre manager Ramesh has initiated and actively managed to deliver over 100 industrial projects within three years of launching of SEAM. His persistence on the quality and on time delivery has seen SEAM grow in strength and it currently serves over 55 companies from wide ranging industrial sectors.

Professor Declan McCormack completed his BA (Moderatorship) in Natural Sciences (Chemistry) at the University of Dublin, Trinity College (TCD), and his PhD in Chemistry/Material Science under the direction of Prof. John Kelly and Prof. Michael Lyons at TCD. He was appointed as lecturer in Physical Chemistry at the Dublin Institute of Technology in 1990 and as Head of School of the School of Chemical & Pharmaceutical Sciences in 2005. He is the Academic Director of the Centre for Research in Engineering Surface Technology (CREST). CREST has won many awards including the Big Ideas showcase commercialisation award in 2009. He is a Fellow of the Royal Society of Chemistry and the Institute of Chemistry in Ireland and is Secretary of the Chemical and Physical Sciences Committee of the Royal Irish Academy.

Leakage or pre-switch region

In this low current region, below the threshold voltage (typically voltage at a corresponding current of $<10^{-4}$ A cm^{-2}), the *I–V* curve shows linear (ohmic) characteristics.[2,3] The resistivity of the varistor is very high here (greater than 10^{10} Ω cm for a normal ZnO varistor) and performs like an open circuit. For a given varistor device, capacitance remains constant over a wide range of voltage and frequency in the pre-switch region and its dielectric characteristics are governed by the impedance of the ZnO grain boundaries.[2,4]

For AC applications, the total leakage current (I_L) in the pre-breakdown region is composed of resistive (I_R) and capacitive (I_C) currents. In the design of a surge suppresser from a ZnO varistor, it is the resistive current (I_R), which is of importance since this is responsible for Joule heating within the elements. The parameters, which are known to influence the leakage current, are (a) formulation of the materials (b) voltage applied and (c) time interval of the voltage applied.[2–30] Leakage current is one of the critical parameters that requires to be considered in the design of an over voltage protector.

Non-linear or varistor operation region

The region between the threshold voltage and a current of 100 A cm^{-2} is considered as the most important part of the varistor action. The *I–V* curve is non-linear in this region wherein the varistor voltage remains approximately constant for a large change in current. The varistor characteristics of this region can be described by the eqn (1.1).[2,3]

$$I = C(V)^{\alpha} \tag{1.1}$$

Here C is the material constant and the exponent α defines the degree of non-linearity. α is regarded as the most significant parameter for the varistor action.[2,3] It can be determined either from the reciprocal slope of the log V–log I curve (Fig. 2) in the nonlinear region[2–6] or calculated from the formula [1.2].

$$\alpha = \log(I_2/I_1)/\log(V_2/V_1) \tag{1.2}$$

where, V_1 and V_2 are voltages at currents I_1 and I_2. The higher the value of non-linearity or α, the better will be the protection of the device. Lagrange[7] has shown that α reaches a maximum near 1 mA cm^{-2}. Because of its variation with current, an α value is normally cited between current ranges of 0.1 to 1 mA cm^{-2}, 1 to 10 mA cm^{-2} or in specific cases up to 100 mA cm^{-2}. Typical reported α values for ZnO varistors range from 20 to 100 over the current ranges mentioned above.[2,3,29] In contrast, varistors developed from other alternative materials such as SiC and TiO_2 do not show α values above 10.[2]

Another critical application parameter for ZnO varistors is the threshold or breakdown voltage (V_c), which marks the transition from linear to nonlinear mode. The voltage at the onset of this nonlinearity, just above the knee of the *I–V* curve, is also known as the nonlinear voltage. In real varistor devices, there is a lack of sharpness of the transition in the *I–V* curve and the exact location of this parameter is often difficult to determine.

High current or upturn region

In this high current region (>100 A cm^{-2}), the varistor approximates to a short circuit. The *I–V* curve exhibits linear characteristics similar to those in the low current region and approaches the value of the material bulk resistivity, about 1–10 Ω cm. The dielectric characteristics of this upturn region are governed by the impedance of the grain in the ZnO microstructure.[2,3,6–10]

In summary, the most desirable characteristics of a varistor include a high value of nonlinear coefficient (α), an acceptable rating of nonlinear voltage (V_c), a low value of leakage current (I_L), a long varistor life and a high-energy absorption capability.[1–4]

Mechanism of varistor action

Pure ZnO without any impurities or dopants is a non-stoichiometric n-type semiconductor with a linear or ohmic behaviour. To make a non-linear material, various metal oxides have to be incorporated into the ZnO.[1,3,5,6] These oxides are added to control one or more of the properties such as the electrical characteristics (breakdown voltage, non-linearity and leakage current), grain growth or sintering temperature.[2,3,45–50] Bi_2O_3 is the most essential component for forming the non-ohmic behaviour and addition of CoO and MnO enhances the non-linear properties.[2–6] A very low concentration of Al_2O_3 increases the ZnO grain conductivity while Sb_2O_3 controls the ZnO grain growth.[31–40,46–57] Combination of additives such as Cr_2O_3, MnO, Bi_2O_3 and CoO, produces greater non-linearity than a single dopant.

During high temperature treatment (sintering) different phases are formed and the microstructure of a ZnO varistor comprises conductive ZnO grains surrounded by electrically insulating grain boundary regions. The first highly nonlinear composition with $\alpha = 50$ was reported by Matsuoka.[1] In addition to 97 mol% ZnO he added 0.5 mol% each of Bi_2O_3, CoO, MnO, Cr_2O_3 and 1 mol% Sb_2O_3. Inada[9] in 1980 reported the formation of chemical phases during the heat treatment in the range 950–1050 °C. The ZnO–Bi_2O_3–Sb_2O_3 system forms a pyrochlore phase $Zn_2Bi_3Sb_3O_{14}$ above 650 °C. With ZnO pyrochlore further reacts to form a spinel ($Zn_7Sb_2O_{12}$).[3,9] This can be readily observed by XRD (Fig. 3).

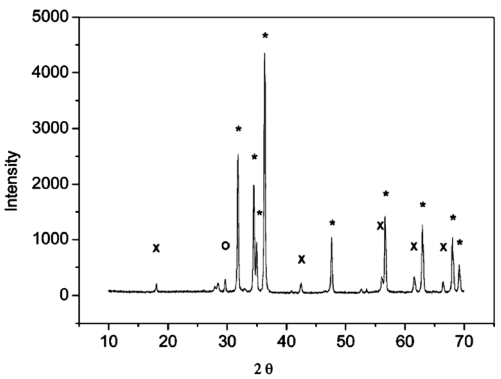

Fig. 3 XRD pattern of a sintered ZnO varistor indicating various components such as * = ZnO; x = $Zn_7Sb_2O_{12}$; o = Bi_2O_3. (Re-produced with permission from S. C. Pillai, J. M. Kelly, D. E. McCormack and R. Ramesh, *J. Mater. Chem.*, 2008, **18**, 3926.)

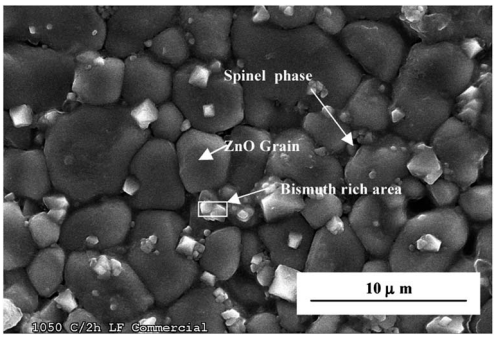

Fig. 4 FESEM image of (a) ZnO grain, spinel ($Zn_7Sb_2O_{12}$) phase and bismuth rich phases of a commercial varistor sample. (S. C. Pillai, J. M. Kelly, D. E. McCormack and R. Ramesh, *J. Mater. Chem.*, 2008, **18**, 3926. *Reproduced with permission*).

$$\underset{\text{(Pyrochlore)}}{2Zn_2Bi_3Sb_3O_{14} + 17ZnO} \xrightarrow{950-1050\,^{\circ}C} \underset{\text{(Spinel)}}{3Zn_7Sb_2O_{12} + 3Bi_2O_3} \quad (1.3)$$

Additive oxides are found predominantly at grain boundaries (Fig. 4). As trapping of charge at the grain boundaries is known to have a major effect on the electrical transport properties, it is important to investigate the microstructure of the materials.[11–30]

The final grain size of a typical commercial varistor after sintering is of the order of 8–12 μm and the corresponding breakdown voltage is around 200–300 V mm^{-1}.[2,3] The breakdown voltage of the sintered body is proportional to the number of grain boundaries. Electron microscopy (SEM) of a typical microstructure clearly shows the presence of grains and regions where other crystalline phases are present (Fig. 4). EDX can be used to identify the elements present (Fig. 5).

Thus the following three major crystalline phases are usually found in a typical varistor microstructure.[2–14,58–67] (a) ZnO grains; (b) $Zn_7Sb_2O_{12}$, spinel crystal structure; (c) bismuth rich phases. These phases could be identified from the XRD pattern (Fig. 3). Spinel and pyrochlore are mainly crystallised in inter-granular phases, while Bi-rich phases are found at the triple points (Fig. 4 and 5).[2,3,68–73]

Arefin *et al.*[68] performed thermodynamic calculations to predict the phase formation, composition and stability of additive oxides during the sintering process of ZnO varistors. They modelled the phase formation during sintering in the Zn–Bi–O and Zn–Bi–Sb–O mixtures (Fig. 6).

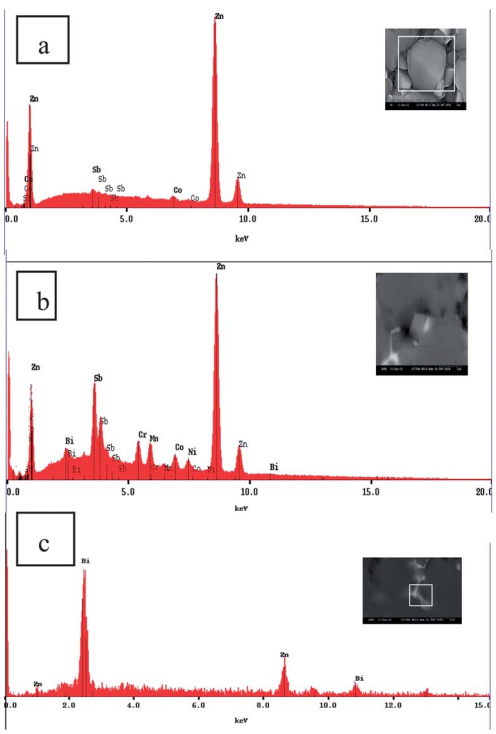

Fig. 5 EDX images of (a) ZnO grains (b) spinel ($Zn_7Sb_2O_{12}$) phase (c) bismuth rich phase (white areas in the microstructure) (*Re-produced with permission from* S. C. Pillai, J. M. Kelly, D. E. McCormack and R. Ramesh, *J. Mater. Chem.*, 2008, **18**, 3926).

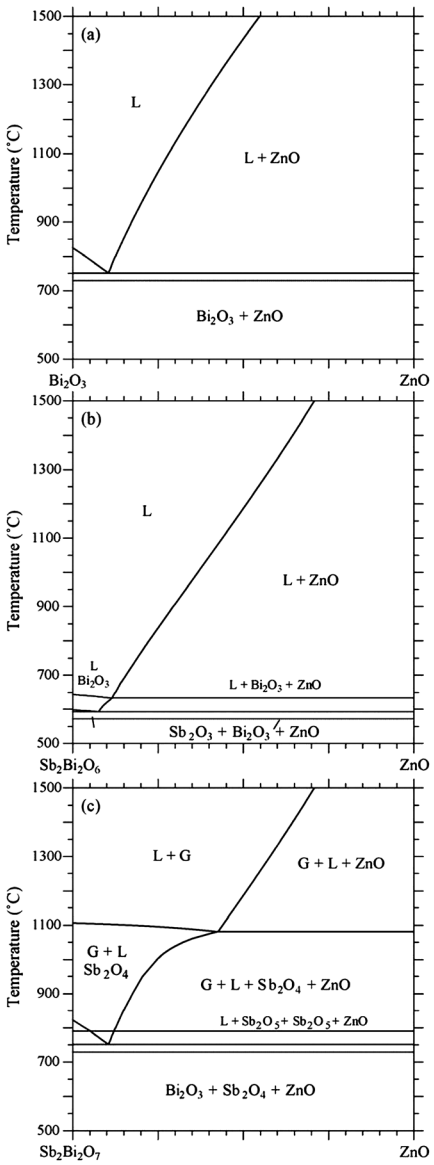

Fig. 6 Thermodynamically calculated temperature-composition sections for (a) ZnO–Bi_2O_3, (b) ZnO–Bi_2O_3–Sb_2O_3 and (c) ZnO–Bi_2O_3–Sb_2O_4 (L = liquid, G = gas) (*Re-produced with permission from* M. L. Arefin, F. Raether, D. Dolejs and A. Klimera, *Ceram. Int.*, 2009, **35**, 3313).

The binary system Bi_2O_3–ZnO is characterised by an asymmetric location of the eutectic at 750 °C and 89 mol% Bi_2O_3. It was also noted that the initial melt only dissolved a small quantity of zinc oxide and therefore the extent of liquid phase in the system is basically controlled by the Bi_2O_3 fraction in the sample. However, Sb_2O_3 incorporation leads to a depression of the solidus from 750 °C to 590 °C (Fig. 6b), because of the comparatively lower melting point of Sb_2O_3. The low temperature melt is dominated by Bi_2O_3/Sb_2O_3 and it contains less than 10 mol% liquefied ZnO. Fig. 6c shows the formation of liquid phase in the Bi_2O_3–Sb_2O_4–ZnO ternary system. It may be noted that the eutectic melting is not depressed below a temperature of 760 °C. Under these conditions, four major phases can be identified such as ZnO, Sb_2O_5, Bi_2O_3/Sb_2O_3 and Sb_2O_4. During sintering various phases in the microstructure are distributed in such a way that the grain boundary region converts to a highly resistive phase ($\rho_{gb} \sim 10^{12}$ Ω cm) and the grain interior becomes highly conductive (ρ_{gb} 1–10 Ω cm). An equivalent electrical circuit of a varistor can be represented as in Fig. 7.[67] A sharp drop in resistivity from grain boundary region to the ZnO grain usually occurs within a space of ~50 to 100 nm. This is normally considered as a depletion layer.[2,9] Thus at each grain boundary area there exists a depletion layer extending into the nearby ZnO grains. The varistor action is believed to be produced as a result of the presence of these depletion layers between the ZnO grains.[2–6]

The grain growth in varistor ceramics occurs by the creation of ZnO–Bi_2O_3 binary structures during the liquid phase sintering process.[2,9,31–44,46–57,68] This formation of bismuth-rich phases has been analysed using XRD, FESEM and EDX analysis (Fig. 3 and 4). It should be noted that bismuth oxide has a comparatively lower melting point (656 °C) and the eutectic liquid temperature for ZnO–Bi_2O_3 binary system is 740 °C. Therefore, a substantial enhancement of grain growth is expected above the eutectic liquid temperature, compared with the grain growth of pure un-doped ZnO.[2,68–73] This is reported as due to the creation of liquid bismuth along the ZnO grain boundaries, which enhances the grain boundary movement and thus facilitates the grain growth.[68–73] These observations further demonstrate that controlling the grain size during sintering at high temperature remains a real challenge in conventional ceramic processing.[69–73] It is possible that other sintering procedures such as step sintering or microwave-assisted sintering might be applied to get a fully sintered varistor disc at a lower temperature.[73,75]

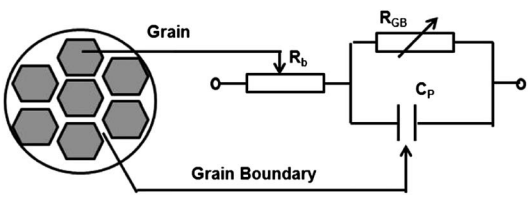

Fig. 7 Equivalent electrical circuit of a varistor component[67] (Re-drawn from reference: E. Savary, S. Marinel, F. Gascoin, Y. Kinemuchi, J. Pansiot and R. Retoux, *J. Alloys Compd.*, 2011, **509**, 6163).

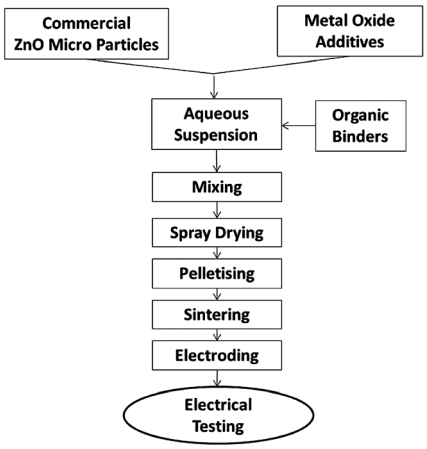

Scheme 1 Stages in conventional industrial processing of varistor ceramics.

Principal industrial synthetic method

ZnO varistors are conventionally prepared by mixing the requisite metal oxide powders and subsequently preparing an aqueous suspension.[2,69–73] The resultant wet powder is mixed with an organic binder (*e.g.* polyvinyl alcohol) and plasticiser (*e.g.* polyethylene glycol), and then spray-dried to get a granulated powder. This powder is hard-pressed into ceramic pellets and then sintered at a temperature of 1100 to 1200 °C. The sintered disc is silver electroded and leads attached prior to encapsulating the disc in an epoxy based polymer.[2]

This type of processing route is still the preferred method in varistor manufacturing plants (Scheme 1). The low cost associated with the use of comparatively inexpensive oxide powders is the main commercial attraction of this route. A major disadvantage of the solid state route is the difficulty in obtaining a compositionally homogeneous micro-structure, which is particularly important for the fabrication of the miniaturised devices required for modern electronic and communication equipment.[69–73]

Need for new processing routes

The phenomenal growth in the production of personal and tablet computers, smart mobile phones and similar electronic devices with rapidly improved performance and miniaturization has generated a consequent increase in demand for ever smaller zinc oxide based varistors.[2–4] As explained in the previous sections, the breakdown voltage of the sintered body is proportional to the number of grain boundaries between the electrodes and an ideal varistor has a crystalline microstructure with grains of uniform size, distribution and composition. Therefore it should be possible to improve the electrical and electronic characteristics of varistors by controlling the microstructure at the grain boundaries.

Microstructural homogeneity is also a key property needed to control the ohmic and non-ohmic behaviour of varistors, as inhomogeneous microstructure can cause degradation of varistors during electrical operation. Thus careful control of the ceramic microstructure is essential to produce a high quality

varistor.[69–76] However, compositional homogeneity is difficult to achieve by conventional ceramic routes involving mechanical milling or grinding. For this purpose chemical processing would seem to offer considerable advantages.[3,70–73]

The probable advantages of using nano-scale materials are illustrated by the report that pure nanophase ZnO can also exhibit varistor behaviour with a small but usable threshold voltage of 100 V mm^{-1} for material with a 60 nm diameter grain size prepared through gas condensation technique.[117] Other authors have shown that doped nanophase ZnO with 3–10 nm grains shows a varistor behaviour with threshold voltages up to 3000 V mm^{-1},[100] demonstrating that it is possible through nanostructuring to produce ZnO varistors with very high threshold voltages by controlling the grain size and hence the number of grain boundaries in the material.[69–74,100]

An additional factor important for the commercial production of varistors is the sintering temperature, which is normally 1100–1300 °C. If this could be reduced, for example by nanostructuring, this would be of considerable economic benefit. It may be noted that the smaller the particle size the lower the temperature required. This arises because the increased surface area causes the particles to flow together at lower temperatures. The reduced sintering temperature has therefore been one of the driving forces behind the use of nanoscale materials.

Major chemical procedures used to prepare varistors

Chemical processing conveniently allows the production of nanoparticulate materials and the homogeneous distribution of dopants. As will be shown below this has been achieved by a number of routes with reactions proceeding in the gas phase, solution phase or by sol–gel methods.

Gas-phase and combustion synthesis

Plasma pyrolysis. Plasma pyrolysis technology has been employed to synthesise nanometer size precursor powders of ZnO.[88] $ZnSO_4$ and NH_4HCO_3 were used as the precursors for the preparation of a $Zn_5CO_3(OH)_6$ intermediate, which was then ultrasonically dispersed in NH_4HCO_3 solution. Nitrates of Sb, Bi, Co, Y and Mn were added to the dispersion. The complex precipitate was further washed, dried and then pyrolysed by plasma. TEM studies showed that the doped ZnO particles were spherical with a size ranging 10 to 50 nm. Varistors were fabricated by sintering the doped ZnO nanomaterial at a temperature of 1050 °C. Scanning electron microscopy (SEM) study showed that the average size of the varistor grain was 1.0 μm. Electrical results revealed a breakdown voltage of 500 V mm^{-1}, a nonlinear coefficient of 54 and a leakage current of 1 μA. The combination of the nanoparticle size, spherical shape and narrow particle size distribution were proposed as the reasons for the decrease in the sintering temperature and enhanced electrical properties. However, despite the superior properties of the material, it is probably expensive to implement on an industrial scale.

Gas discharge activated reaction evaporation. Another approach to the production of varistor nano-material is the use of a gas discharge activated reaction evaporation technique (GDARE) to prepare high quality ZnO varistor films.[127] In this method the synthetic parameters are simple to optimise and desired properties can be obtained by changing the preparation parameters. Finely ground zinc powder is vaporised in a molybdenum boat. A high voltage is applied between this evaporation source and the ITO or glass substrate. The plasma thus produced activates the oxygen gas present, which then reacts with the zinc vapour, forming a ZnO film on the substrate. AFM studies showed that the thin films have polycrystalline structures with grain sizes ranging from 50 to 200 nm (Fig. 8). The α value of a single coated thin film is 33 and that of a triple-coated sample is reported as 62. It was concluded that the ZnO thin films prepared by GDARE consists of a higher number of varistor active grain boundaries capable of absorbing oxygen which effectively generates many electronic trapping states, leading to the creation of Schottky barriers at the grain boundary region. It is interesting that these good performance characteristics were obtained without the addition of dopants and the method should be promising for small scale devices.[127]

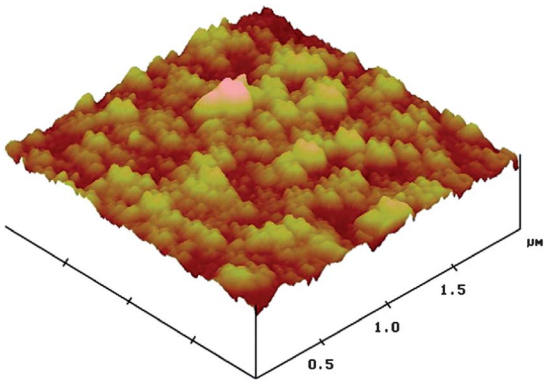

Fig. 8 AFM image of a ZnO varistor thin film sample prepared by the GDARE technique (*reproduced with permission* L. Hui, W. Yuele, L. Xian, *Mater. Lett.*, 2009, **63**, 2321).

Combustion synthesis. The basis of the combustion synthesis technique comes from the thermochemical concepts used in the field of propellants and explosives.[83,84] It uses reactants that oxidise easily (such as nitrates) and a stable organic fuel (*e.g.* urea, glycine *etc.*) that acts as a reducing agent.[84,126] The mixture is heated until it ignites and a self-sustaining and rather swift combustion reaction takes place, resulting in a dry fine non-agglomerated powder. Using this method pure and doped ZnO powders were synthesised from mixtures of the relevant water soluble metal nitrates and urea as fuel.[83] The mixtures were ignited at 500 °C resulting in the varistor precursor with particle sizes ranging from 52 to 158 nm, suggesting that this material might be useful for varistor production. However, no electrical results were reported.[83]

In 2011, Hembram *et al.*[125] synthesised varistor powders in the size range between 15 and 250 nm by a modified chemical combustion route. The doped nanocrystalline ZnO nanopowder was prepared using sucrose as a fuel. The process is straightforward and is proposed to be suitable for industrial scale production as it involves short processing time. After sintering, electrical studies indicated a breakdown voltage of 950 V mm^{-1}

and non-linear coefficient of 134. This study demonstrates the feasibility of a single step preparation of doped ZnO varistor materials with improved performances.

Other ZnO nanopowders have also been prepared by combustion synthesis using glycine as a fuel and zinc nitrate as an oxidant and zinc source. Varistor discs were produced after sintering at 1050 °C for 1.5 h. A good nonlinear coefficient of 42, a breakdown voltage of 205 V mm^{-1} and low leakage current (1.15 A) were obtained. However the sintered density was rather low (92%).[126]

Liquid phase synthesis

Solution processing is another means of creating nanoparticles and also of manipulating precursors to form bulk oxide materials.[69–78,89–96] The advantages of wet chemical processing are primarily the higher purity and homogeneity and the lower processing temperature.[3,71–73] Multi-component dopant oxides can also be readily prepared by mixing relevant salt solutions of metal salts.[3,73] By wet chemical methods homogeneity of the dopant ions among the ZnO grains can be achieved at the atomic level. The temperature required for sintering also depends on the particle size and homogeneous distribution of dopants among the individual grains.[3,71–74] A number of liquid phase approaches have been followed as outlined below.

Precipitation reactions. An aqueous precipitation technique for the synthesis of spherical ZnO particles (eqn (1.4)) was used by Haile *et al.*[79]

$$\begin{aligned} &ZnSO_4\cdot 7H_2O + NH_4OH \rightarrow \\ &\quad xZnSO_4\cdot yZn(OH)_2\cdot 2H_2O \xrightarrow{H_2O/pH=9/heat} \\ &\quad Zn(OH)_2 + (NH_4)_2SO_4 + NH_3 \xrightarrow{55\,^{\circ}C} ZnO \end{aligned} \quad (1.4)$$

Coating of the ZnO powders was achieved by precipitation of dopant chlorides such as $BiCl_3\cdot H_2O$, $CoCl_3\cdot 6H_2O$, $MnCl_2\cdot 4H_2O$, $CrCl_3\cdot H_2O$ and SbCl using an aqueous solution of $(NH_4)CO_3$. This procedure allowed the fabrication of varistors with properties comparable to conventionally fabricated varistors (nonlinear coefficient of 44 and a breakdown voltage of 180 V mm^{-1}).

Nanosize ZnO between 3 and 10 nm prepared by a reaction between zinc perchlorate ($Zn(ClO_4)_2$) and sodium hydroxide in methanol under a nitrogen atmosphere have also been used for the preparation of varistors.[100] Precipitation and centrifugation methods were used to collect the resultant powders. The nano powder thus obtained was doped with Bi, Sb, Co, B, Sn and Cu oxides. The material produced has a remarkably high breakdown voltage of 3000 V mm^{-1} with a nonlinear exponent α of 50. Similar ZnO varistor materials were prepared by a co-precipitation route with the objective to develop a low-voltage ZnO varistor.[101] Reagents such as ZnO, $Bi(NO_3)_3$, $MnCl_2\cdot 4H_2O$, $Co(NO_3)_2\cdot 6H_2O$, $Ni(NO_3)_2\cdot 9H_2O$, $Ti(C_2H_5O)_4$ and $Sn(NO_3)_2\cdot 3H_2O$ were used as precursors. Metal salts were dissolved in hydrochloric acid and precipitated by ammonium bicarbonate. A breakdown voltage of 87.5 V mm^{-1} and a nonlinear coefficient of 32.5 were reported.

Other ultra-fine ZnO nanoparticles for varistor applications have been prepared by a two-step precipitation reaction.[102] In the first step zinc sulphate ($ZnSO_4$) was reacted with ammonia to obtain zinc hydroxide ($Zn(OH)_2$). Then, in the second step, the above product was mixed with ammonium bicarbonate (NH_4HCO_3) to produce hydrozincite ($Zn_5(OH)_6(CO_3)_2$) precipitate. After aging and washing, these materials were annealed at 450 °C to obtain ZnO nanoparticles. These nanoparticles were further mixed with Bi_2O_3, MnO_2, Sb_2O_3, Cr_2O_3 and Co_2O_3 and sintered at 1200 °C for two hours. A breakdown voltage of 492 V mm^{-1} with a non-linear coefficient (α) of 56 was obtained. This method is inexpensive and has good potential for scale-up.

Precipitation reactions in organic solvents have also been used to prepare nano-composite varistor powders.[103] The dopants were dissolved in a mixture of ethylene glycol and ethanol and added to the above solution. To this reaction mixture ZnO was added and ultra-sonicated for one hour. It was dried at 150 °C for 8 h and subsequently calcined at 450 °C to obtain ZnO particles covered with oxides of dopants. The composite materials were further annealed at 600 °C to obtain the varistor powder. The agglomerated varistor powder thus obtained was pulverised, pelletised and sintered at 1050 °C. These varistors showed a breakdown voltage (V_c) of 540 V mm^{-1} and a nonlinear coefficient (α) of 50.[103]

Amine processing. A varistor powder preparation method involving amines as precipitants has been reported.[78] ZnO, Bi_2O_3, $SbCl_3$, $CoCl_2$ were dissolved in hydrochloric acid, and diethylamine solution added to co-precipitate all the components. The resulting mixture was washed, dried and calcined to produce active and uniform composition powders of small particle size (200 nm). High nonlinearity coefficients ($\alpha = 50$) and breakdown voltage (711 V mm^{-1}) were achieved in varistors fabricated from these powders prepared by sintering in the range 1100 °C to 1250 °C. This sintering temperature is significantly lower than many conventional industrial manufacturing (1200–1300 °C) but higher than other laboratory procedures. The amine process is found to be a good method for preparing uniform powders of doped-ZnO for varistor production.

Citrate gel synthesis. Citrate gel processes have been employed successfully to prepare varistor materials by several groups.[76,80–84,99] A typical procedure involves the production of solid amorphous precursors by the dehydration of gels, produced by the addition of citric acid to a solution of nitrate salts of zinc and the dopant metals. The solid precursors are subsequently decomposed and oxidised in air to yield the oxide materials. The technical advantage of this method is high chemical homogeneity in the resulting powder and the simplicity of the procedure. Therefore it is a promising method for the preparation of ZnO varistor powders.[80–84,99] For example Fan and Sale[80] prepared ZnO varistors from the resultant oxide powder, which had submicron particle size. They reported a breakdown voltage of 400 V mm^{-1} and nonlinear coefficient of 20. These improved electrical properties has been explained by the chemically more homogeneous microstructures obtained in the gel processed material. Other authors[81] reported a similar method yielding a nano-powder (37 nm), which sintered to a high density (98%) in one hour at 1150 °C. The resultant

varistors exhibited a reasonably high non-linear coefficient (35), low leakage current (11.1 μA) and a high breakdown voltage of 515 V mm^{-1}. Similarly, Duran and co-workers[76] successfully synthesised nano-sized (~28 nm) ZnO based ceramic powders. A dense ceramic was fabricated by normal liquid phase sintering at 850 °C and 940 °C for 1 to 5 hours. Electrical studies showed a high non-linear coefficient (70) and a high breakdown voltage (1500 V mm^{-1}).

Micro-emulsion synthesis. ZnO powders for varistor applications have been prepared by mixing two micro-emulsions.[85–87] These were prepared using the surfactant CTAB (cetyl trimethyl ammonium bromide), 1-butanol as co-surfactant, *n*-octane as continuous 'oil' phase and aqueous solutions of the reagents in the dispersed phase. One micro-emulsion contained zinc nitrate, while the other contained the precipitating agent $(NH_4)_2CO_3$.[86] The ZnO produced had a particle size of 14 nm. The varistor dopants were added by precipitation yielding a device after sintering at 1200 °C, with a nonlinear coefficient of 83 and a breakdown voltage of 450 V mm^{-1}.[86]

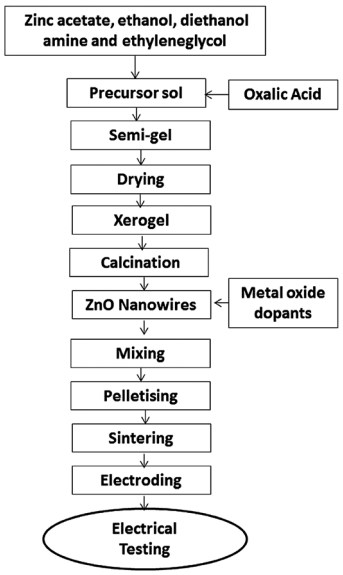

Scheme 2 Flowchart for the preparation of ZnO nanowires for varistor applications (Re-drawn: reference S. C. Pillai, J. M. Kelly, D. E. McCormack and R. Ramesh, *J. Mater. Chem.*, 2004, **14**, 1572).

Sol–gel processing

As discussed in previous sections, varying the microstructure at the grain boundary regions can alter varistor properties.[121] Sol–gel processing provides a method for homogeneous doping at the molecular level[3,70–73,118,119] which is very important in varistors since inhomogeneous distribution of dopants in a varistor results in the formation of hot spots as the current follows the path of least resistance and may lead to the failure of the varistor at a lower current than the expected value. The benefit of homogeneous chemical processing[3,69] has been demonstrated by comparing the varistor properties of sol–gel materials to those of devices prepared by solid state mixing all of the metallic oxide precursors and solid phase oxalic acid. Although calcination and sintering of these materials were carried out under identical conditions, electrical studies identified that these latter materials did not show any acceptable varistor action.[3] This observation was attributed to the inhomogeneity of the additives distributed among the ZnO grains.[3,69–73]

Sol–gel processing involves stages such as sol formation, gelling, creation of the xerogel, calcination and drying.[122] There are several reports available in the literature where ZnO prepared through sol–gel techniques have been used for varistor applications.[3,71–73,97–99,104–111] In general two different approaches have been taken, the first involving, the sol–gel preparation of ZnO and the subsequent addition of solid dopant metal oxides and secondly, the preparation of the gel from the precursor solutions of the zinc and metal additives.

An example of the first approach is the work of Pillai *et al.*[3,69–73] where the preparation of nanoparticles and nanowires using novel sol–gel synthetic procedures is described (Scheme 2). ZnO precursor gels were initially prepared by the reaction of an ethanolic solution of zinc acetate and ethanolic solution of oxalic acid. The gel was then dried at 80 °C calcined at 500 °C for two hours. This produced ZnO nanoparticles of size 30 nm. In a further experiment two chemical modifiers (ethylene glycol and diethanolamine) were added to the ethanolic solution of zinc acetate before the addition of the ethanolic solution of oxalic acid. The gel formed was subsequently treated as above and the powder characterised by XRD, FESEM and TEM. FESEM revealed a fibrous structure containing elongated bundles of 100 nm widths and 2–4 μm lengths. Further ultra-sonication for 40 minutes separated the individual wires from the bundle.

TEM studies showed that these wires were composed of spherical nanoparticles of 21 nm. The 500 °C annealed wires were further calcined to 1000 °C and FESEM studies showed that the individual particles were sintered together to form continuous wires of width 0.3 to 0.4 μm and 10 to 20 μm length (Fig. 9).

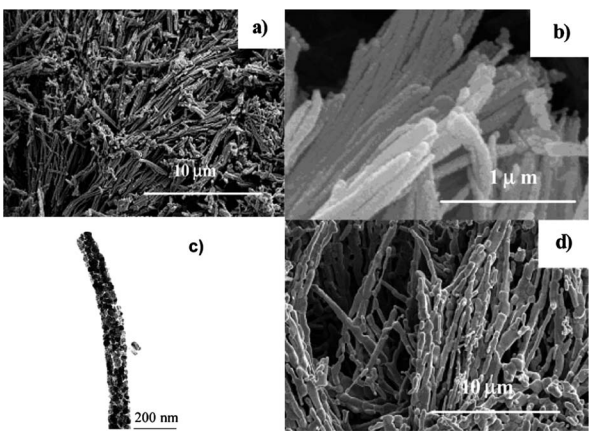

Fig. 9 Electron microscopy images of nanowire ZnO for varistor applications prepared by a sol–gel route. (a) and (b) FESEM after calcination at 500 °C; (c) TEM of a single array of ZnO nanoparticle separated by ultrasonication in ethanol; (d) FESEM of nano-array ZnO calcined at 1000 °C (Re-produced with permission from S. C. Pillai, J. M. Kelly, D. E. McCormack and R. Ramesh, *J. Mater. Chem.*, 2004, **14**, 1572).

The precursor morphologies and formation mechanisms were studied in detail by TEM, FTIR and thermal analysis. Two of the above materials were doped with commercial metal oxides using a conventional solid state mixing technique and a core–shell type doped varistor (where ZnO was the core and the dopants formed a shell) was also made using spherical ZnO nanoparticles and metal salts as additives.[71] Sintering (1050 °C for two hours) and electrical studies were carried out for each of these samples and the results compared with commercial varistor samples pelletised and sintered under the same conditions. Core–shell type samples showed considerably higher breakdown voltage compared to the other nano samples mixed with commercial additives made under similar conditions.

FESEM analysis (Fig. 10) indicated a smaller average grain size (1.5 μm) for "core–shell" samples compared to the commercial varistors (3 μm). Even though the electrical properties were superior (Table 1), only 97% densification was achieved at 1050 °C for two hours (A densification greater than 99% is recommended by industrial requirements).

Westin and co-workers[104–106] have tried different sol–gel methods to obtain the varistor precursors and have determined microstructural and electrical properties. Typical sol–gel precursors used were $Ni(OAc)_2 \cdot 4H_2O$, $Co(OAc)_2 \cdot 4H_2O$, $Mn(OAc)_2 \cdot 4H_2O$, $Cr_3(OAc)_7(OH)_2$, $Al(NO_3)_3 \cdot 9H_2O$, $Sb(OBu^n)_3$ and bi(2-ethylhexanoate)$_3$. A breakdown voltage of 249 V mm^{-1} and $\alpha = 37$ are obtained for one such varistor material.[105] These useful properties for the sol–gel processed material are consistent with homogeneous mixing of the additive oxides on the ZnO grains.[105] In other studies, Ya *et al.*[107,108] reported the fabrication of varistors using sol–gel prepared ZnO nanopowders (20 nm). These materials displayed superior electrical properties with a high value of the nonlinear coefficient ($\alpha = 45$) and lower leakage current ($I_L < 1$ μA). Puyane *et al.* also reported the production of ZnO powders by a sol–gel route and showed that these sintered at lower temperatures compared to the conventional varistor materials.[109,110]

Another sol–gel method was developed by Hohenberger and Tomandl.[111] Two sets of salt solutions were initially prepared. The first involved hot water containing the acetates of Zn, Co, and Mn, and H_3BO_3 and the second was an ethyleneglycol solution of Sb-acetate, Cr-nitrate, Bi-nitrate and Al-nitrate. Mixing and cooling generates a microcrystalline gel of the precursor materials. Solvent was removed by freeze drying and the remaining powder annealed at 450 °C before pelletising and sintering at 1100 °C. Satisfactory electrical behaviour ($\alpha = 55$, and breakdown voltage 375 V mm^{-1}) was recorded.

Table 1 Various synthesis procedures for varistors and comparison of the electrical characteristics

Synthetic route	Sintering (°C)	V_c (V mm^{-1})	α
Solid phase			
Plasma pyrolysis			
Lin[88]	1050	500	54
Combustion			
Hembram[125]	1050	205	42
Citrate gel			
Fan[80]	1200	400	20
Sinha[81]	1150	515	35
Duran[76]	850	1500	70
Precursor-mixing			
Pillai[69]	1050	656	—
Liquid phase			
Amine processing			
Hishita[78]	1050	711	50
	1200	339	52
	1300	256	36
Precipitation			
Haile[79]	1200	180	44
Viswanath[100]	750	3000	50
Wang[101]	—	87	32
Yang[102]	1200	492	56
Li[103]	1050	540	50
Core–shell			
Pillai[71]	1050	850	33
Micro-emulsion			
Hingorani[86]	1200	450	83
Sol–gel			
Pillai[72]	1050	786	34
Pillai[3]	1050	859	33
Westin[104–106]	1100	249	37
Puyane[109]	1100	—	12
Puyane[110]	1100	259	—
Tomandl[111]	1100	375	60
Ya[107,108]	950	1000	45
Lauf[113]	1000	980	30
Nobrega[114]	1100	800	26
Chu[115,116]	1000	—	50
Commercial formulation[a]			
Pillai[3,69,71,72]	1050	507	48

[a] Industrial sintering temperature usually varies between 1050 and 1200 °C.

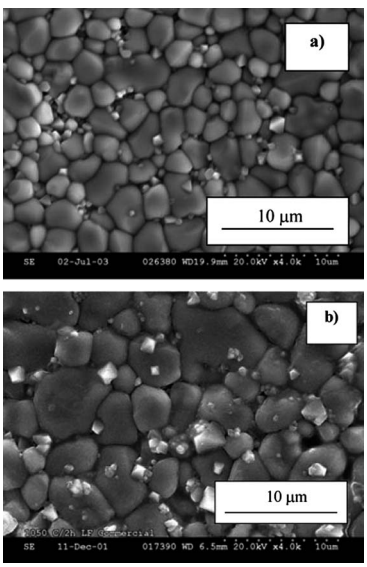

Fig. 10 FESEM images of the sintered varistor samples (a) sol–gel samples (b) commercial samples. *Reproduced with permission* S. C. Pillai, J. M. Kelly, D. E. McCormack, P. O'Brien and R. Ramesh, *J. Mater. Chem.*, 2003, **13**, 2586.

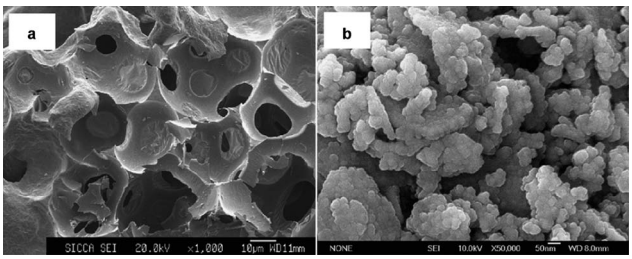

Fig. 11 SEM micrograph of the xerogel (a) and ZnO powder (b) prepared by sol–gel method (*Reproduced with permission*: L. H. Cheng, L. Y. Zheng, L. Meng, G. R. Li, Y. Gu, F. P. Zhang, R. Q Chu, Z. J Xu, *Ceram. Int.*, 2012, **38S**, S457).

Very recently Cheng *et al.*,[128] reported the preparation of sol–gel based Al_2O_3-doped ZnO varistors with high performance. The powder prepared from the xerogel (Fig. 11a) after annealing was loosely agglomerated (Fig. 11b) and the individual particle size was uniformly in the range of 30–40 μm. Addition of Al_2O_3 was found to be essential to achieve optimum properties. The average grain size after sintering decreased from 4.4 μm to 3.0 μm and the breakdown voltage increased from 720 V mm^{-1} to 1160 V mm^{-1} as the amount of Al_2O_3 increased from 0.0 wt% to 0.40 wt%. Again improved varistor properties of these ZnO materials are credited to the smaller grain size distribution due to the sol–gel process.[128]

A large-scale sol–gel based processing route, which could produce a fully dense varistor at a lower temperature with superior electrical properties has been also reported.[3] The method involves the use of soluble metal salts, oxalic acid, diethanolamine and ethyleneglycol in ethanol solution.[3] Unlike many of the above mentioned laboratory methods, this particular route proposed is easily scaled up for the production of nanomaterials for fabrication of high performance varistors. Furthermore, these materials showed a higher breakdown voltage compared to the other reported methods and exhibited a high densification at a temperature, which is 150 °C less than the commercial standard sample.[13] A considerably larger breakdown voltage (V_c) was also reported (Fig. 12) for these samples (941 V mm^{-1}) compared to commercial samples (507 V mm^{-1}).[69,71]

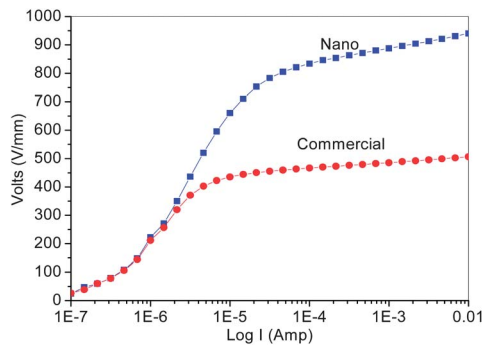

Fig. 12 Varistor samples prepared by sintering at 1050 °C (*Reproduced with permission*: S. C. Pillai, J. M. Kelly, D. E. McCormack, R. Ramesh, *J. Mater. Chem.*, 2008, **18**, 3926).

As detailed above (and in other reports),[112–116] sol–gel methods produce superior electrical properties. A selection of these are compared to those of other methods in Table 1. It may also be noted that chemical processing methods offer considerable benefits compared to the traditional industrial procedure. However, these advantages may be offset by (a) longer processing time (b) comparatively higher cost of the metal oxide precursors and (c) large amount of solvents required for synthesis.[3,70,71]

Grain growth during sintering. Sintering behaviour of the varistor discs prepared from nano samples has been studied by densification, grain growth and dilatometric studies (Fig. 13). Density measurements indicated that the sintered density value increased considerably at 900 °C.[3] The dilatometric results (Fig. 13c) showed that the onset of sintering occurred in the range 875–925 °C and is complete in the range 1025–1050 °C. Grain growth studies showed that the particles have increased considerably at 900 °C compared to 800 °C. This study also confirmed that the sintering process and grain growth occurred simultaneously (Fig. 13b).

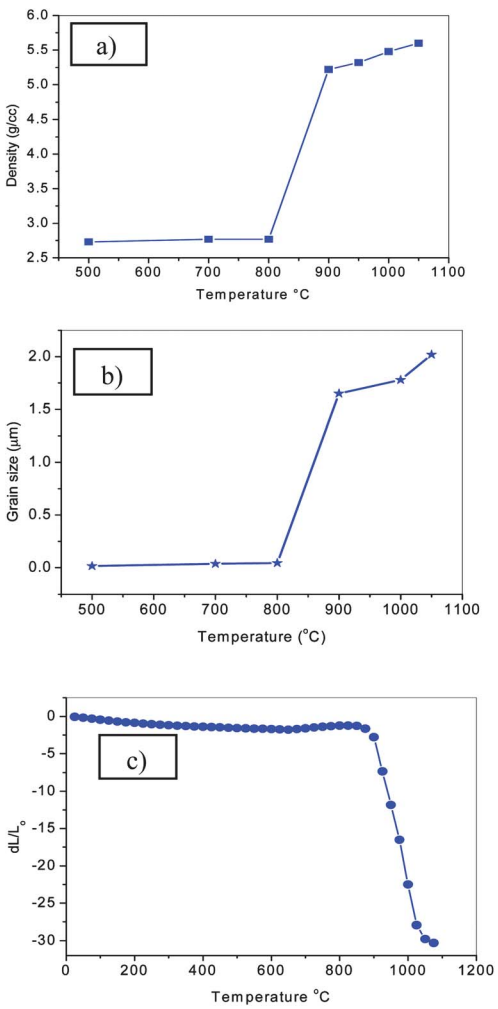

Fig. 13 Change in density and grain size of varistor discs at high temperature (a) change in density with temperature (b) grain size *vs.* temperature (c) dilatometer curve of varistor nanopowder (*Reproduced with permission*: S. C. Pillai, J. M. Kelly, D. E. McCormack and R. Ramesh, *J. Mater. Chem.*, 2008, **18**, 3926).

Therefore, irrespective of preparation routes, the grain growth at high sintering temperature still remains a significant challenge for developing miniaturised varistor devices. New sintering procedures have therefore been recently developed to obtain sub-micron grain size with optimum electrical characteristics.

New sintering methods to control grain growth in varistor materials. It should be noted that the breakdown voltage might be increased several-fold if one could sinter the material to full density with sub-micron grain size. A good approach to this is step-sintering[73] which may allow the production of a fully sintered varistor disc at a lower temperature. This method employs two or more steps in the heating schedule. The ceramic disc is initially heated in a furnace at a higher temperature to achieve a reasonably good density, then cooled down and retained at a slightly lower temperature for several hours. In a typical step-sintering process, the samples were heated to 1000 °C, then allowed to cool for over 30 min to 900 °C and held there for 6 hours.[73] Such a step sintering procedure has been tried for the preparation of varistor materials.[73,75–77] For example, a sintered density higher than 99%, sub-micron grain size and superior electrical properties (breakdown voltage 2050 V mm^{-1} and $\alpha =$ 96) can be obtained.[75]

Additionally, microwave sintering methods have received much attention in recent years.[77,120,123,124] The major advantage of microwave based sintering is that it is more rapid than conventional sintering and the grain growth can be controlled.[67] Therefore, unlike the conventional heating process, the microwave assisted processing provides an energy efficient, green and convenient method of producing ceramic materials.[129–133] Savary *et al.*[67] have prepared a nano-sized ZnO-based varistor powder by a chemical processing route and sintered it within a short time in either conventional or microwave furnaces for comparison. It was shown that the microwave heating enhanced the overall density and the reaction kinetics between the different phases. ZnO varistors sintered using microwave energy also showed significantly improved electrical properties and enhanced densification.[67] A better distribution of dopants and homogeneous supply of temperature among the bulk of the ceramics are also reported as unique features of microwave sintering (Fig. 14).

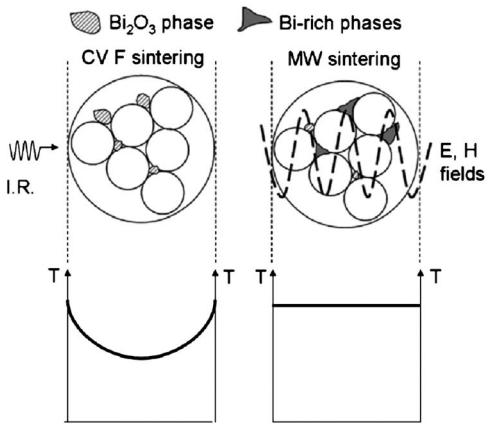

Fig. 14 Comparison of varistor sintering in a conventional furnace and in a microwave furnace (Re-produced with permission: E. Savary, S. Marinel, F. Gascoin, Y. Kinemuchi, J. Pansiot and R. Retoux, *J. Alloys Compd.*, 2011, **509**, 6163).

Spark plasma sintering (SPS) or pulsed electric current sintering (PECS) technique is also a powerful methodology to sinter ZnO varistors.[134–138] SPS combines the application of both pressure and pulsed DC current directly on the ceramic sample.[134–136] The low-voltage DC pulse transiently produces spark plasma at high temperatures between particles. The role of the DC pulse in the plasma formation and its impact on sintering mechanism is still a subject of controversy.[134] However, the method is found to be highly effective in sintering ZnO nanomaterials for varistor applications.[135–138] For example Macary *et al.*,[137] employed the SPS technique to sinter ZnO–Bi_2O_3 nanomaterial (10 nm) at temperatures ranging from 550 to 600 °C. The grain size of such materials sintered at 600 °C was reported as 300 to 500 nm with breakdown voltage of 1066 V mm^{-1} and an α value of 5.8. A reasonably high density of 97% is also obtained for the sintered discs at 600 °C.[137] The α value of 5.8 is not satisfactory for any varistor ceramics, but it can be improved by incorporating other metal oxides such as MnO, CoO *etc.*[3,69–73] Therefore, the SPS technique shows some potential as a sintering method for developing ZnO materials with desirable varistor properties.

Further future investigations in the area of step-sintering, microwave sintering and spark plasma sintering are expected to deliver varistors with significantly improved electrical properties.

Conclusions

While the solid-state based ceramic processing route still remains the preferred method of manufacturing because of the simplicity, cost and availability of the metal oxide additives, this process has considerable disadvantages especially for many modern commercial applications. A major disadvantage of this route is the difficulty in obtaining additive homogeneity at a microscopic level, which is especially important for the manufacture of miniaturised electronic equipment. Processing methods and additive homogeneity are the critical parameters to produce a varistor material with favourable electrical characteristics. Inhomogeneous microstructures could cause degradation of varistors during electrical operation. Therefore, careful control of the microstructure is required to produce a varistor of desired characteristics. As shown in the sections above, and in Table 1, chemical processing (such as sol–gel, solution, precipitation, micro-emulsion techniques *etc.*) facilitates a homogeneous doping at the molecular level. Among the various methods reported, sol–gel processing is found to be a promising procedure to obtain a miniature device with higher breakdown voltage, low leakage current and reasonably good non-linear characteristics. However, controlling the grain growth at high sintering temperatures still remains a challenge for varistor ceramics and the electrical properties could be improved, if the materials could be sintered to full density with sub-micrometer or nanometer grain size. Indeed, a significant enhancement in electrical properties has been achieved by

novel sintering procedures such as step sintering, spark plasma sintering or using microwave irradiation. Further development of such methods is anticipated in the near future.

References

1 M. Matsuoka, *Jpn. J. Appl. Phys.*, 1971, **10**, 736.
2 T. K. Gupta, *J. Am. Ceram. Soc.*, 1990, **73**, 1817.
3 S. C. Pillai, J. M. Kelly, D. E. McCormack and R. Ramesh, *J. Mater. Chem.*, 2008, **18**, 3926.
4 (*a*) D. R. Clarke, *J. Am. Ceram. Soc.*, 1999, **82**, 485; (*b*) K. Eda, *IEEE Electr. Insul. Mag.*, 1989, **5**, 28.
5 (*a*) J. Fan and R. Freer, *Br. Ceram. Trans.*, 1993, **96**, 221; (*b*) T. Asokan and R. Freer, *J. Mater. Sci.*, 1990, **25**, 2447.
6 D. C. Look, *Mater. Sci. Eng., B*, 2001, **80**, 383.
7 A. Lagrange, *Electronics ceramics*, ed. B. C. H. Steele, Elsevier Applied Science London and New York, 1991, p. 17.
8 R. Einzinger, *Annu. Rev. Mater. Sci.*, 1987, **17**, 299.
9 M. Inada, *Jpn. J. Appl. Phys.*, 1980, **19**, 409.
10 L. M. Levinson and H. R. Philip, *Ceram. Bull.*, 1986, **165**, 639.
11 S. A. Shojaee, M. M. Shahraki, M. A. F. Sani, A. Nemati and A. Yousefi, *J. Mater. Sci.: Mater. Electron.*, 2010, **21**, 571.
12 G. D. Mahan, L. M. Levinson and H. R. Philipp, *J. Appl. Phys.*, 1979, **50**, 2799.
13 L. M. Levinson and H. R. Philipp, *IEEE Transactions on Parts, Hybrids, and Packaging*, 1977, **13**, 338.
14 R. Einzinger, *Appl. Surf. Sci.*, 1979, **3**, 390.
15 L. M. Levinson and H. R. Philipp, *J. Appl. Phys.*, 1979, **50**, 383.
16 S. Fujitsu, H. Toyoda and H. Yanagida, *J. Am. Ceram. Soc.*, 1987, **70**, C71–C72.
17 R. A. Winston and J. F. Cordaro, *J. Appl. Phys.*, 1990, **68**, 6495.
18 H. L. Tuller, *J. Electroceram.*, 1999, **4**, 33–40.
19 J. P. Han, A. M. R. Senos and P. Q. Mantas, *Mater. Chem. Phys.*, 2002, **75**, 117.
20 Y. Suzuoki, A. Ohki, T. Mizutani and M. Ieda, *J. Phys. D: Appl. Phys.*, 1987, **20**, 511.
21 E. Olsson, G. L. Dunlop and R. Osterlund, *J. Appl. Phys.*, 1989, **66**, 5072.
22 N. Raghu and T. R. N. Kutty, *Appl. Phys. Lett.*, 1992, **60**, 100.
23 C. W. Nahm, C. H. Park and H. S. Yoon, *J. Mater. Sci. Lett.*, 2000, **19**, 271.
24 B. A. Haskell, S. J. Souri and M. A. Helfand, *J. Am. Ceram. Soc.*, 1999, **82**, 2106.
25 E. Suvaci and I. O. Ozer, *J. Eur. Ceram. Soc.*, 2005, **25**, 1663.
26 Z. Brankovic, G. Brankovic, D. Poleti and J. A. Varela, *Ceram. Int.*, 2001, **27**, 115.
27 M. Peiteado, *Bol. Soc. Esp. Ceram. Vidrio*, 2005, **44**, 77.
28 L. F. Lou, *Appl. Phys. Lett.*, 1980, **36**, 570.
29 S. Ezhilvalavan and T. R. N. Kutty, *Mater. Chem. Phys.*, 1997, **49**, 258.
30 L. Hui, W. Yuele and L. Xian, *Mater. Lett.*, 2009, **63**, 2321.
31 X. L. Fu, W. H. Tang and Z. J. Peng, *Acta Phys. Sin.*, 2008, **57**, 5844.
32 M. Bartkowiak, G. D. Mahan, F. A. Modine and M. A. Alim, *J. Appl. Phys.*, 1996, **79**, 273.
33 J. P. Han, A. M. R. Senos and P. Q. Mantas, *J. Eur. Ceram. Soc.*, 2002, **22**, 1653.
34 Y. Kaiyang, L. Guorong and Z. Liaoying, *J. Alloys Compd.*, 2010, **503**, 507.
35 T. R. N. Kutty and N. Raghu, *Appl. Phys. Lett.*, 1989, **54**, 1796.
36 J. Ott, A. Lorenz, M. Harrer, E. A. Preissner, C. Hesse, A. Feltz, A. H. Whitehead and M. Schreiber, *J. Electroceram.*, 2001, **6**, 135.
37 J. M. Carlsson, B. Hellsing, H. S. Domingos and P. D. Bristowe, *J. Phys.: Condens. Matter*, 2001, **13**, 9937.
38 K. Shu-Ting, T. Wei-Hsing, S. Jay and S. F. Wang, *J. Eur. Ceram. Soc.*, 2007, **16**, 4521.
39 (*a*) J. Fan and R. Freer, *J. Mater. Sci.*, 1993, **28**, 1391; (*b*) A. Sedky, T. A. El-Brolossy and S. B. Mohamed, *J. Phys. Chem. Solids*, 2012, **73**, 505.
40 S. Bernik and N. Daneu, *J. Eur. Ceram. Soc.*, 2007, **27**, 3161.
41 W. Mao-Hua, H. Ke-Ao and Z. Bin-Yuan, *Mater. Chem. Phys.*, 2006, **100**, 142.
42 H. Chen and G. Fu, *Solid-State Electron.*, 2012, **67**, 27.
43 W. C. Long, J. Hu, J. Liu and J. L. He, *Mater. Lett.*, 2010, **64**, 1081.
44 C. Peng-Fei, Li S. -Tao and L. Jian-Ying, *Acta Phys. Sin.*, 2010, **59**, 560.
45 J. L. He, J. Hu and J. Y. H. Lin, *Sci. China, Ser. E: Technol. Sci.*, 2008, **51**, 693.
46 N. Daneu, A. Recnik and S. Bernik, *J. Eur. Ceram. Soc.*, 2011, **94**, 1619.
47 C. Leach, N. K. Ali, D. Cupertino and R. Freer, *Mater. Sci. Eng., B*, 2010, **170**, 15.
48 M. Mehdi, A. M. Zahedi and S. K. Sadrnezhaad, *J. Am. Ceram. Soc.*, 2008, **91**, 56.
49 D. Dey and R. C. Brad, *J. Eur. Ceram. Soc.*, 1992, **75**, 2529.
50 J. P. Gambino, W. D. Kingery, G. E. Pike, H. R. Philipp and L. M. Levinson, *J. Appl. Phys.*, 1987, **61**, 2571.
51 D. R. Clarke, *J. Appl. Phys.*, 1979, **50**, 6829.
52 A. P. Hynes, R. H. Doremus and R. W. Siegel, *J. Am. Ceram. Soc.*, 2002, **85**, 1979.
53 M. Peiteado, J. F. Fernandez and A. C. Caballero, *J. Am. Ceram. Soc.*, 2005, **25**, 2999.
54 S. Anas, R. Metz, M. A. Sanoj, R. V. Mangalaraja and S. Ananthakumar, *Ceram. Int.*, 2010, **36**, 2351.
55 R. Subasri, M. Asha, K. Hembram, G. V. N. Rao and T. N. Rao, *Mater. Chem. Phys.*, 2009, **115**, 677.
56 S. T. Kuo, W. H. Tuan, Y. W. Lao, C. K. Wen and H. R. Chen, *J. Am. Ceram. Soc.*, 2008, **91**, 1572.
57 L. Yeh-Wu, K. Shu-Ting and T. Wei-Hsing, *J. Electroceram.*, 2007, **19**, 187.
58 H. R. Chen, Y. R. Wang, C. Y. Chang, R. T. Chang, T. L. Tsai, Y. W. Lao, S. T. Kuo, C. L. Hsieh and W. H. Tuan, *J. Electroceram.*, 2008, **21**, 361.
59 A. Recnik, S. Bernik and N. Daneu, *J. Mater. Sci.*, 2012, **47**, 1655.
60 A. Vojta and D. R. Clarke, *J. Appl. Phys.*, 1997, **81**, 985.
61 R. Aleksander, B. Slavko and D. Nina, *J. Mater. Sci.*, 2012, **47**, 1655.

62 O. I. Ozguer, S. Ender and B. Slavko, *Acta Mater.*, 2010, **58**, 4126.
63 C. Leach, N. K. Ali, D. Cupertino and R. Freer, *Mater. Sci. Eng., B*, 2010, **170**, 15.
64 S. A. Shojaee, M. M. Shahraki, M. A. F. Sani, A. Nemati and A. Yousefi, *J. Mater. Sci.: Mater. Electron.*, 2010, **21**, 571.
65 P. Wen-Hsuan, K. Shu-Ting, T. Wei-Hsing and Huey-Ru Chen, *Int. J. Appl. Ceram. Technol.*, 2010, **7**, E80–E88.
66 K. Shu-Ting and T. Wei-Hsing, *J. Eur. Ceram. Soc.*, 2010, **30**, 525.
67 E. Savary, S. Marinel, F. Gascoin, Y. Kinemuchi, J. Pansiot and R. Retoux, *J. Alloys Compd.*, 2011, **509**, 6163.
68 M. L. Arefin, F. Raether, D. Dolejs and A. Klimera, *Ceram. Int.*, 2009, **35**, 3313.
69 S. C. Pillai, J. M. Kelly, D. E. McCormack and R. Ramesh, *Mater. Sci. Technol.*, 2004, **20**, 964.
70 G. Duffy, S. C. Pillai and D. E. McCormack, *J. Mater. Chem.*, 2007, **17**, 181.
71 S. C. Pillai, J. M. Kelly, D. E. McCormack, P. O'Brien and R. Ramesh, *J. Mater. Chem.*, 2003, **13**, 2586.
72 S. C. Pillai, J. M. Kelly, D. E. McCormack and R. Ramesh, *J. Mater. Chem.*, 2004, **14**, 1572.
73 S. C. Pillai, J. M. Kelly, D. E. McCormack and R. Ramesh, *Adv. Appl. Ceram.*, 2006, **105**, 158.
74 E. A. Gusa, I. Teoreanu, A. Petrescu, M. Ionescu and M. Barladeanu, *Rev. Rom. Mater.*, 2009, **39**, 57.
75 M. M. Shahraki, S. A. Shojaee, M. A. F. Sani, A. Nemati and I. Safaee, *Solid State Ionics*, 2011, **190**, 99.
76 P. Duran, F. Capel, J. Tartaj and C. Moure, *J. Am. Ceram. Soc.*, 2001, **84**, 1661.
77 J. G. P. Binner, I. Caro and J. Firkins, *J. Microw. Power. Electromagn. Energy*, 1999, **34**, 131.
78 S. Hishita, Y. Yao and S.-I. Shirasaki, *J. Am. Ceram. Soc.*, 1989, **72**, 338.
79 S. M. Haile, D. W. Johnson, Jr, G. H. Wiseman and H. K. Bowen, *J. Am. Ceram. Soc.*, 1989, **72**, 2004.
80 J. Fan and F. R. Sale, *Electroceramics Production, Properties and Microstructure*, ed W. E. Lee and A. Bell, The Institute of Materials, London, 1994, p. 151.
81 A. Sinha and B. P. Sharma, *Mater. Res. Bull.*, 1997, **32**, 1571.
82 A. Banarjee, T. R. Rammohan and M. J. Ptani, *Mater. Res. Bull.*, 2001, **36**, 1259.
83 V. C. Sousa, A. M. Segadaes, M. R. Morelli and R. H. G. A. Kiminami, *Int. J. Inorg. Mater.*, 1999, **1**, 235.
84 S. R. Dhage, S. C. Navale and V. Ravi, *Ceram. Int.*, 2007, **33**, 289.
85 M. Singhal, V. Chhabra, P. Kang and D. O. Shah, *Mater. Res. Bull.*, 1997, **32**, 239.
86 S. Hingorani, V. Pillai, P. Kumar, M. S. Multani and D. O. Shah, *Mater. Res. Bull.*, 1993, **28**, 1303.
87 S. Hingorani, D. O. Shah and M. S. Multani, *J. Mater. Res.*, 1995, **10**, 461.
88 Y. Lin, Z. Zhang, Z. Tang, F. Yuan and J. Li, *Adv. Mater. Opt. Electron.*, 1999, **9**, 205.
89 L. H. Cheng, G. R. Li, L. Y. Zheng, J. T. Zeng, Y. Gu and F. P. Zhang, *J. Am. Ceram. Soc.*, 2010, **93**, 2522.
90 K. Z. Monsef, S. Mohammad and A. M. Asadi, *Synth. React. Inorg., Met.-Org., Nano-Met. Chem.*, 2011, **41**, 814.
91 Y. Huang, M. Liu, Z. Li, Y. Zeng and S. Liu, *Mater. Sci. Eng., B*, 2003, **97**, 111.
92 S. Y. Chu, T. M. Yan and S. L. Chen, *J. Mater. Sci. Lett.*, 2000, **19**, 349.
93 K. Hembram, D. Sivaprahasam and T. N. Rao, *J. Eur. Ceram. Soc.*, 2011, **31**, 1905.
94 L. Meng, L. Y. Zheng, L. H. Cheng, G. R. Li, L. Z. Huang, Y. Gu and F. P. Zhang, *J. Mater. Chem.*, 2011, **21**, 11418.
95 S. Komarneni, M. Bruno and E. Mariani, *Mater. Res. Bull.*, 2000, **35**, 1843.
96 C. F. Jin, X. Yuan, W. W. Ge, J.-M. Hong and X.-Q. Xin, *Nanotechnology*, 2003, **14**, 667–669.
97 E. Sonder, T. C. Quinby and D. L. Kinser, *Am. Ceram. Soc. Bull.*, 1986, **65**, 665.
98 S. Arman and N. N. Riyahi, *J. Ceram. Process. Res.*, 2011, **12**, 752.
99 N. Riahi-Noori, R. Sarraf-Mamoory, P. Alizadeh and A. Mehdikhani, *J. Ceram. Process. Res.*, 2008, **9**, 246.
100 R. N. Viswanath, S. Ramasamy, R. Ramamoorthy, P. Jayavel and T. Nagarajan, *Nanostruct. Mater.*, 1995, **6**, 993.
101 M. H. Wang, C. Yao and N. F. Zhang, *J. Mater. Process. Technol.*, 2008, **202**, 406.
102 W. Yang, D. Zhou, G. Yin and R. Wang, *J. Mater. Process. Technol.*, 2005, **21**, 183.
103 Y. Li, G. Li and Q. Yin, *Mater. Sci. Eng., B*, 2006, **130**, 264.
104 G. Westin and M. Nagren, *J. Mater. Chem.*, 1993, **3**, 367.
105 G. Westin, A. Ekstrand, M. Nagren, R. Osterlund and P. Merkelbach, *J. Mater. Chem.*, 1994, **4**, 615.
106 A. Ekstrand, M. Nagren and G. Westin, *J. Sol–Gel Sci. Technol.*, 1997, **8**, 697.
107 K. X. Ya, H. Yin, T. M. De and T. M. Jing, *Mater. Res. Bull.*, 1998, **33**, 1703.
108 K. X. Ya, W. T. Diao, H. Yin, T. M. De and T. M. Jing, *Mater. Res. Bull.*, 1998, **32**, 1165.
109 R. Puyane, F. Toal and S. Hampshire, *J. Sol–Gel Sci. Technol.*, 1996, **6**, 219.
110 R. Puyane, I. Guy and R. Metz, *J. Sol–Gel Sci. Technol.*, 1998, **13**, 575.
111 G. Hohenberger and G. Tomandl, *J. Mater. Res.*, 1992, **7**, 546.
112 L. Kong, F. Li, L. Zhang and X. Yao, *J. Mater. Sci. Lett.*, 1998, **17**, 769.
113 R. T. Lauf and W. D. Bond, *Am. Ceram. Soc. Bull.*, 1984, **2**, 278.
114 M. C. S. Nobrega, M. S. Zolotar, W. A. Mannheimer and A. Espinola, *J. Non-Cryst. Solids*, 1992, **147–148**, 803.
115 S. Y. Chu, T.-M. Yan and S.-L. Chen, *J. Mater. Sci. Lett.*, 2000, **19**, 349.
116 S. Y. Chu, T.-M. Yan and S.-L. Chen, *Ceram. Int.*, 2000, **26**, 733.
117 J. T. Lee, J.-H. Hawang, J. J. Mashek, T. O. Mason, A. E. Miller and R. W. Siegel, *J. Mater. Res.*, 1995, **10**, 2295.
118 C. D. Chandler, C. Roger and J. Hampden-Smith, *Chem. Rev.*, 1993, **93**, 1205.

119 S. Anas, R. V. Mangalaraja, M. Poothayal, S. K. Shukla and S. Ananthakumar, *Acta Mater.*, 2007, **55**, 5792.
120 R. Roy, D. Agrawal, J. Cheng and S. Gedevanishvili, *Nature*, 1999, **399**, 668.
121 S. Bernik, G. Brankovic, S. Rustja, M. Zunic, M. Podlogar and Z. Brankovic, *Ceram. Int.*, 2008, **34**, 1495.
122 S. W. Boland, S. C. Pillai, W.-D. Yang and S. M. Haile, *J. Mater. Res.*, 2004, **19**, 1492.
123 R. Subasri, M. Asha, K. Hembram, G. V. N. Rao and T. N. Rao, *Mater. Chem. Phys.*, 2009, **115**, 67.
124 B. Vaidhyanathan, K. Annapoorani, J. Binner and R. Raghavendra, *J. Am. Ceram. Soc.*, 2010, **93**, 2274.
125 K. Hembram, D. Sivaprahasam and T. N. Rao, *J. Eur. Ceram. Soc.*, 2011, **31**, 1905.
126 C.-C. Hwang and T.-Y. Wu, *Mater. Sci. Eng., B*, 2004, **111**, 197.
127 H. Lu, Y. Wang and X. Lin, *Mater. Lett.*, 2009, **63**, 2321.
128 L. H. Cheng, L. Y. Zheng, L. Meng, G. R. Li, Y. Gu, F. P. Zhang, R. Q. Chu and Z. J. Xu, *Ceram. Int.*, 2012, **38S**, S457.
129 P. Periyat, N. Leyland, D. E. McCormack, J. Colreavy, D. Corr and S. C. Pillai, *J. Mater. Chem.*, 2010, **20**, 3650.
130 S. C. Padmanabhan, D. Ledwith, S. C. Pillai, D. E. McCormack and J. M. Kelly, *J. Mater. Chem.*, 2009, **19**, 9250.
131 D. Ledwith, S. C. Pillai, G. Watson and J. M. Kelly, *Chem. Commun.*, 2004, 2294.
132 D. W. Synnott, M. K. Seery, S. J. Hinder, J. Colreavy and S. C. Pillai, *Nanotechnology*, 2013, **24**, 45704.
133 D. W. Synnott, M. K. Seery, S. J. Hinder, G. Michlits and S. C. Pillai, *Appl. Catal., B*, 2013, **130–131**, 106.
134 T. Hungria, J. Galy and A. Castro, *Adv. Eng. Mater.*, 2009, **11**, 615.
135 I. Lorite, M. A. Rodriguez, F. Azough, R. Freer and J. F. Fernandez, *J. Am. Ceram. Soc.*, 2012, **95**, 1023.
136 L. Gao, Q. Li, W. Luan, H. Kawaoka, T. Sekino and K. Niihara, *J. Am. Ceram. Soc.*, 2002, **85**, 1016.
137 L. S. Macary, M. L. Kahn, C. Estournès, P. Fau, D. Trémouilles, M. Bafleur, P. Renaud and B. Chaudret, *Adv. Funct. Mater.*, 2009, **19**, 1775.
138 Z. Shen and M. Nygren, *Chem. Rec.*, 2005, **5**, 173.